

Quantitative Analysis of Glutamate Receptors in Glial Cells from the Cortex of GFAP/EGFP Mice Following Ischemic Injury: Focus on NMDA Receptors

David Dzamba^{1,2} · Pavel Honsa¹ · Martin Valny¹ · Jan Kriska^{1,2} · Lukas Valihrach³ · Vendula Novosadova³ · Mikael Kubista³ · Miroslava Anderova¹

Received: 21 April 2015 / Accepted: 15 May 2015 / Published online: 21 May 2015
© Springer Science+Business Media New York 2015

Abstract Cortical glial cells contain both ionotropic and metabotropic glutamate receptors. Despite several efforts, a comprehensive analysis of the entire family of glutamate receptors and their subunits present in glial cells is still missing. Here, we provide an overall picture of the gene expression of ionotropic (AMPA, kainate, NMDA) and the main metabotropic glutamate receptors in cortical glial cells isolated from GFAP/EGFP mice before and after focal cerebral ischemia. Employing single-cell RT-qPCR, we detected the expression of genes encoding subunits of glutamate receptors in GFAP/EGFP-positive (GFAP/EGFP⁺) glial cells in the cortex of young adult mice. Most of the analyzed cells expressed mRNA for glutamate receptor subunits, the expression of which, in most cases, even increased after ischemic injury. Data analyses disclosed several classes of GFAP/EGFP⁺ glial cells with respect to glutamate receptors and revealed in what manner their expression correlates with the expression of glial markers prior to and after ischemia. Furthermore, we also examined the protein expression and functional significance of NMDA

receptors in glial cells. Immunohistochemical analyses of all seven NMDA receptor subunits provided direct evidence that the GluN3A subunit is present in GFAP/EGFP⁺ glial cells and that its expression is increased after ischemia. In situ and in vitro Ca²⁺ imaging revealed that Ca²⁺ elevations evoked by the application of NMDA were diminished in GFAP/EGFP⁺ glial cells following ischemia. Our results provide a comprehensive description of glutamate receptors in cortical GFAP/EGFP⁺ glial cells and may serve as a basis for further research on glial cell physiology and pathophysiology.

Keywords Astrocytes · NG2 glia · MCAo · Single-cell RT-qPCR · Calcium imaging

Introduction

The era when glial cells were considered to be just passive bystanders of neuronal transmission was supplanted by a new era in which they are seen to actively communicate with neurons and participate in crucial processes, including the development of the nervous system, synaptic plasticity, and synaptogenesis. Glial cells of ectodermal origin are divided according to their function into astrocytes, NG2 glia (also called polydendrocytes or oligodendrocyte precursor cells—OPCs), oligodendrocytes, and ependymal cells. In this work, we studied GFAP/EGFP⁺ glial cells, which mostly comprise astrocytes; however, there are indications of NG2 glia overlap, especially in juvenile animals (Matthias et al. 2003; Serrano et al. 2008).

Similarly to neurons, glial cells possess a variety of metabotropic and ionotropic glutamate receptors. Metabotropic glutamate receptors (mGluR1–8) regulate various intracellular signal cascades, and several of these

Electronic supplementary material The online version of this article (doi:10.1007/s10571-015-0212-8) contains supplementary material, which is available to authorized users.

✉ Miroslava Anderova
anderova@biomed.cas.cz

¹ Present Address: Department of Cellular Neurophysiology, Institute of Experimental Medicine, Academy of Sciences of the Czech Republic, Videnska 1083, Prague 4, Czech Republic

² 2nd Faculty of Medicine, Charles University, Prague, Czech Republic

³ Laboratory of Gene Expression, Institute of Biotechnology, Academy of Sciences of the Czech Republic, Prague, Czech Republic

receptors have been identified in astrocytes, with mGluR3 and mGluR5 being the most abundant (Verkhratsky 2009; Loane et al. 2012). Ionotropic glutamate receptors are divided according to their specific agonists into three groups—AMPA, kainate, and NMDA. They differ in their subunit composition, functional properties such as desensitization rate or specificity in ion permeability, and also in their different occurrence in various brain cell types depending on the CNS region. AMPA receptor subunits (GluA1–4) are present in astrocytes in most brain regions (Seifert and Steinhäuser 2001), and their subunit composition determines their Ca^{2+} permeability (Hollmann et al. 1991; Burnashev et al. 1992). All kainate receptor subunits (GluK1–5) have been identified in astrocytes either on the mRNA or protein level (Brand-Schieber et al. 2004); however, the functional properties of these receptors have not been demonstrated so far. The last group of astrocytic glutamate receptors is NMDA receptors composed of GluN1–3B subunits, which is a highly debatable receptor family with a large therapeutic potential (for review see Verkhratsky and Kirchhoff 2007; Dzamba et al. 2013). In contrast to neuronal NMDA receptors, they do not possess a Mg^{2+} block (Lalo et al. 2006; Castillo et al. 2013), so they are also functional at resting membrane potential, which is probably due to their specific combination of subunits, including the most recently discovered GluN3A and GluN3B subunits. The impact of ischemia on NMDA receptors has been studied in hippocampal astrocytes (Gottlieb and Matute 1997; Krebs et al. 2003), but to the best of our knowledge, there are currently no data regarding cortical astrocytes after ischemia; therefore, we specifically focused on these receptors.

In this work, we used single-cell gene expression profiling, which is a novel and powerful method enabling us to study the correlation of transcript levels among individual cells (Ståhlberg and Bengtsson 2010), which is not possible using classical bulk samples composed of a large number of cells. The goal of this work was to characterize GFAP/EGFP-positive (GFAP/EGFP⁺) cells in the cortex of GFAP/EGFP mice after focal cerebral ischemia and to present a detailed overall picture of glutamate receptors in individual GFAP/EGFP⁺ glial cells with a main focus on NMDA receptors.

Materials and Methods

Induction of Focal Ischemic Injury in GFAP/EGFP Mice: Permanent Middle Cerebral Artery Occlusion (MCAo) Model

The experiments were performed on GFAP/EGFP transgenic mice [line designation TgN(GFAPEGFP)], in which

the expression of EGFP is controlled by the human GFAP promoter (Nolte et al. 2001). All procedures involving the use of laboratory animals were performed in accordance with the European Communities Council Directive 24 November 1986 (86/609/EEC) and animal care guidelines approved by the Institute of Experimental Medicine, Academy of Sciences of the Czech Republic (Animal Care Committee on April 17, 2009; approval number 85/2009 and 036/2012).

Before the induction of focal ischemia, adult mice were anesthetized with 1.5 % isoflurane (Abbot, IL, USA) and maintained in 1 % isoflurane using a vaporizer (Tec-3, Cyprane Ltd., UK). A skin incision between the orbit and the external auditory meatus was made, and a hole (1–2 mm in diameter) was drilled through the frontal bone 1 mm rostral to the fusion of the zygoma and the squamosal bone and about 3.5 mm ventral to the dorsal surface of the brain. The dura was opened, gently removed, and the exposed middle cerebral artery was occluded by a short coagulation with bipolar tweezers (SMT, Czech Republic) at a proximal location, followed by transection of the vessel to ensure permanent occlusion. During the surgery, heating pad was used to maintain the mouse's body temperature at $37 \pm 1^\circ\text{C}$ (Honsa et al. 2012).

Preparation of Cell Suspensions from the Cortex of GFAP/EGFP Mice

Before the collection of single GFAP/EGFP⁺ cells utilizing flow cytometry, the cortical tissue was dissociated using papain treatment. In the experiment, the cells were collected from uninjured mice (5 mice, 63–108 days old; 246 cells), mice 7 days after MCAo (4 mice, 57–64 days old; 199 cells), and mice 14 days after MCAo (3 mice, 64 days old; 126 cells). The animals were deeply anesthetized with pentobarbital (PTB, 100 mg/kg, i.p.; Sigma-Aldrich, MO, USA) and perfused transcardially with cold (4–8 °C) isolation buffer containing (in mM) NaCl 136.0, KCl 5.4, HEPES 10.0, glucose 5.5, and osmolality 290 ± 3 mOsm/kg. To isolate the cerebral cortex, a part of the brain (+2 to –2 mm rostro-caudally from bregma) was sliced into 400- μm coronal sections using an HM650V vibrating microtome (MICROM International GmbH, Germany), and the dorsal cerebral cortex was carefully dissected out from the ventral white matter tracks. In mice after MCAo, the ischemic core with its surrounding tissue (cca 1/2 of the injured hemisphere) was used. The tissue was incubated with continuous shaking at 37 °C for 45–60 min in 5 ml of a papain solution (20 U/ml) and 0.2 ml DNase (both from Worthington, NJ, USA) prepared in isolation buffer. After papain treatment, the tissue was mechanically dissociated by gentle trituration using a 1-ml pipette. According to the manufacturer's instructions, the dissociated cells were

layered on top of 5 ml of ovomucoid inhibitor solution and harvested by centrifugation ($140\times g$ for 6 min). Cell aggregates were removed by filtering with a 30- μm cell strainer (Becton–Dickinson, NJ, USA), and the cells were kept on ice until sorting. This method routinely yielded $\sim 2 \times 10^6$ cells per mouse brain.

Collection of Single GFAP/EGFP⁺ Cells by Flow Cytometry

The collection of single cells was performed using flow cytometer (BD Influx, CA, USA), which was manually calibrated to deposit single cells in the center of each well of 96-well plates (Life Technologies, CA, USA) that were placed on a pre-cooled rack. Only viable and GFAP/EGFP⁺ cells were collected. The viability of the cells was checked using Hoechst 33258 (Life Technologies). Single cells were collected into 5 μl nuclease-free water with bovine serum albumin (1 mg/ μl ; Fermentas, IL, USA) and RNaseOut (20 U; Life Technologies). Collected cells in 96-well plates were stored at -80°C immediately after sorting.

Single-Cell Gene Expression Profiling of Mouse Astrocytes

The gene expression profiling of single GFAP/EGFP⁺ glial cells was performed according to the protocol described in (Rusnakova et al. 2013). Briefly, RNA from single cells was transcribed into cDNA in the wells of 96-well plates. To increase the sensitivity of RT-qPCR, the cDNA from one-half of the cells were first pre-amplified. Subsequently, such pre-processed samples were analyzed for the expression of 25 genes of interest (for primer sequences see (Rusnakova et al. 2013), *Grin3b* forward primer TGGTCGGGGACAAGACATTT, reverse primer TCCGTGTGGAGTGGTAGGTG) using the BioMark qPCR platform (Fluidigm, San Francisco, CA, USA). Data were analyzed in GenEx v.6 software (MultiD, Sweden) utilizing the Kohonen self-organizing maps (SOM) method and principal component analysis (PCA), which divided all cells into three subpopulations according to the expression of these 25 genes. The Spearman correlation coefficients between genes were calculated in SAS v.9.3 software using all data, including the managed off-scale data. Only correlation coefficients for genes having a p value <0.05 are presented in the results.

Immunohistochemistry

The mice were deeply anesthetized with PTB (100 mg/kg, i.p.) and perfused transcardially with 20 ml of saline followed by 20 ml of cooled 4 % paraformaldehyde (PFA) in

0.1 M phosphate buffer. Brains were dissected out, post-fixed for 18 h, and placed stepwise in solutions with gradually increasing sucrose concentrations (10, 20, 30 %) for cryoprotection. Coronal 30- μm -thick slices were prepared using a microtome (HM550, Microm International, Germany). The slices were incubated with 5 % Chemiblocker (Millipore, MA, USA) and 0.2 % Triton in phosphate-buffered saline. This blocking solution was also used as the diluent for the antisera. The slices were incubated with the primary antibodies at $4-8^\circ\text{C}$ overnight, then the secondary antibodies were applied for 2 h. As primary antibodies, we used anti-GluN1 (1:500; Abcam, Cambridge, UK, AB28669), anti-GluN2A (1:400; Abcam, AB106957), anti-GluN2B (1:400; Abcam, AB65875), anti-GluN2C (1:400; Alomone Labs, Jerusalem, Israel, AGC-018), anti-GluN2D (1:400; Alomone Labs, AGC-020), anti-GluN3A (1:400; Abcam, AB111226), and anti-GluN3B (1:500; Abcam, AB35677). As the secondary antibody, we used goat anti-rabbit IgG conjugated with Alexa Fluor 594 (1:200; Molecular Probes, CA, USA, A-11012). The slices were mounted using Aqua Poly/Mount (Polysciences Inc., Germany). All chemicals were purchased from Sigma-Aldrich, unless otherwise stated.

A Zeiss 510DUO LSM confocal microscope equipped with Arg/HeNe lasers was used for immunohistochemical analysis. Stacks of consecutive confocal images taken at intervals of 3 μm were acquired sequentially with two lasers to avoid cross-talk between fluorescent labels. The background noise of each confocal image was reduced by averaging four image inputs. For each image stack the gain and detector offset were adjusted to minimize saturated pixels, yet still permit the detection of weakly stained cell processes. Colocalization images were made using a Zeiss LSM Image Browser.

Preparation of Primary Cultures

Primary cultures of GFAP/EGFP⁺ glial cells were prepared from 40- to 57-day-old mice, either uninjured or those 13–14 days after MCAo. The animals were deeply anesthetized with PTB (100 mg/kg, i.p.) and perfused transcardially with cold ($4-8^\circ\text{C}$) NMDG isolation solution containing (in mM) 110 NMDG-Cl, 2.5 KCl, 24.5 NaHCO_3 , 1.25 Na_2HPO_4 , 0.5 CaCl_2 , 7 MgCl_2 , and 20 glucose (pH 7.4, osmolality 290 mOsm/kg). The brain was sliced into 200- μm coronal sections as described above, and the cortical tissue was dissected out. In mice 14 days after MCAo, the dissected tissue consisted of the ischemic core and its surrounding tissue (cca 1/2 of the injured hemisphere). The isolated tissue was transferred into 1 ml of artificial cerebrospinal fluid (aCSF) solution containing (in mM) 122 NaCl, 3 KCl, 1.3 MgCl_2 , 1.5 CaCl_2 , 28 NaHCO_3 , 1.25 Na_2HPO_4 , and 10 glucose (pH 7.4,

osmolality 305 mOsm/kg), which was supplemented with 0.05 % trypsin (Life technologies), and incubated with continuous shaking at 37 °C for 30 min. After incubation, the tissue was transferred into 1 ml of trypsin inhibitor (Sigma-Aldrich) and dissociated by gentle trituration using a 1-ml pipette. Subsequently, the cells were plated in a volume of 0.15 ml onto 6 coverslips in a 24-well plate, and 0.5 ml of fresh cultivation medium was added into each well. The cultivation medium consisted of high-glucose Dulbecco's Modified Eagle Medium (Life Technologies) supplemented with 15 % fetal bovine serum (PAA Laboratories GmbH, Austria), 2 mM L-glutamine (Sigma-Aldrich), and antibiotic–antimycotic containing penicillin, streptomycin, and amphotericin B (Life Technologies). Cells were cultured in an incubator (100 % humidity, 5 % CO₂) at 37 °C for 5–6 days without medium exchange.

Calcium Imaging Measurements

In situ measurements were performed in the somatosensory cortex of 35–59-day-old GFAP/EGFP mice, either uninjured or mice 13–14 days after MCAo. Transversal brain slices (200 µm thick) were cut in cold (4–8 °C) NMDG isolation solution using a vibration microtome and were kept at room temperature in aCSF solution. The slices were then mounted in a microscope superfusion chamber, which was continually perfused with HEPES-based aCSF containing (in mM) 135 NaCl, 2.7 KCl, 1 MgCl₂, 2.5 CaCl₂, 1 Na₂HPO₄, 10 Glucose, and 10 HEPES (pH 7.4, osmolality 305 mOsm/kg, equilibrated with O₂) at a flow rate of 2.5 ml/min. The regions with GFAP/EGFP⁺ cells, which were 10–20 µm below the surface of the slice, were then found and their positions were recorded. The loading procedure was performed at room temperature in the measurement chamber for 40 min in 3 ml of HEPES-based aCSF (the flow was interrupted during this period) containing 1 µM OGB-1 AM with 0.02 % Pluronic F-127 and continually bubbled with O₂ to avoid ischemic conditions. After the loading, the flow of HEPES-based aCSF was reestablished and the measurements were performed with the cells found prior to the loading. The solutions [*N*-methyl-D-aspartate (NMDA), L-glutamic acid (glutamate), glycine, memantine hydrochloride (memantine), NBQX, and PPADS from Sigma-Aldrich, Germany; DL-2-amino-5-phosphonovaleric acid (DL-APV) from Ascent Scientific, UK; and tetrodotoxin (TTX) from Alomone labs, Israel] were applied through a capillary with an i.d. of 250 µm located 0.5–1 mm from the measurement region and connected to a Perfusion Pressure Kit pressurized application system with a flow rate of 600 µl/min controlled by a ValveBank II controller (AutoMate Scientific, Inc., Berkeley, CA, USA). The HEPES-based aCSF was applied via the application system throughout the entire experiment

to ensure that the Ca²⁺ responses were not influenced by the application itself and to accelerate the solution exchange in the vicinity of recorded cells. OGB-1 fluorescence was detected with a TILL Photonics Imaging System installed on a Zeiss Axioskop 2 FS Plus microscope equipped with a long-distance ×40 objective (IR Achroplan 0.8 W, Zeiss, Germany). A digital camera (PCO Sensicam, Kelheim, Germany) was controlled by TILLVISION software. The excitation light (488 nm) was generated by a Polychrome V (TILL Photonics GmbH, Gräfelfing, Germany), filtered by a BP 450–490 excitation band-pass filter, reflected by a FT 510 beam splitter, and the emitted light was filtered by a LP 515 long-pass filter (Filter Set 09, Zeiss, Germany). Images were acquired at 0.83 Hz and were analyzed offline. Fluorescence intensity (*F*) was measured in the cell bodies and expressed after background correction as $F - F_b$, where F_b was the background fluorescence intensity in the proximity of the analyzed cell. The baseline $F - F_b$ signal was then normalized to 100 %, and the area under the curve was measured during 1 min from the onset of application (expressed in arbitrary units). For measuring the delay of the response, the signal threshold for Ca²⁺ responses in situ was 200 % of the amplitude of the noise signal, and the responses were taken into account only if they occurred within 1 min from the onset of application.

In vitro Ca²⁺ imaging measurements were performed similarly to in situ measurements with the exception of the OGB-1 AM loading procedure. Coverslips with 5–6-day-old cell cultures were incubated for 45 min in 0.5 ml of cultivation medium containing 1.5 µM OGB-1 AM and 0.03 % Pluronic F-127 (Life Technologies) at 37 °C in an incubator (100 % humidity, 5 % CO₂). Fluorescence intensity (*F*) was measured in the cell bodies, if not stated otherwise, and the area under the curve was measured from fluorescence intensity *F* during 1 min from the onset of application (expressed in arbitrary units). Since noise signal in Ca²⁺ imaging in vitro was minimal, for measuring the delay of the response, the threshold for Ca²⁺ responses was set to 120 % of the baseline fluorescence, and responses were taken into account only if they occurred within 1 min from the onset of application.

Results

In this study, GFAP/EGFP⁺ glial cells isolated from the cortices of GFAP/EGFP mice were studied in young adult uninjured mice (controls) and in mice 7 and 14 days after MCAo. Employing a single-cell RT-qPCR technique, we were able to detect changes in the expression of the genes coding particular subunits of glutamate receptors following ischemia. For this purpose, the cells were isolated using

papain dissociation, sorted on a flow cytometer according to their EGFP fluorescence and individually analyzed by single-cell analysis.

Expression Profile of Glutamate Receptor Subunits in Uninjured and Post-ischemic Mouse Brains

At first, we analyzed the incidence of GFAP/EGFP⁺ cells expressing the genes of particular ionotropic glutamate receptor subunits of the AMPA (*Gria1-4*), kainate (*Grik1-5*), and NMDA (*Grin1-3b*) types and of metabotropic glutamate receptors (*Grm1,3,5*) in controls and mice 7 and 14 days after MCAo (Fig. 1). The majority of GFAP/EGFP⁺ cells (567 out of 571) expressed typical astrocytic markers, such as *Slc1a3*, *Glul*, *Gfap*, or *Aqp4*. Four cells, which expressed only markers of NG2 glia (*Cspg4* and/or *Pdgfra*) and did not express any astrocytic marker (*Slc1a3*, *Glul*, *Gfap*, and *Aqp4*), were excluded from the analysis; however, this did not lead to any substantial changes in the gene expression profiling.

The lowest expression from all AMPA receptor subunits was found with the *Gria1* gene, which was expressed only in 2 % of cells isolated from controls (control cells). In cells isolated from mice 7 and 14 days after induction of MCAo (D7 and D14 cells), the incidence of cells expressing the *Gria1* gene was higher, but did not exceed 12 %. Very interesting results were obtained in the case of the *Gria2* gene, which was present in numerous control

cells (61 %) with no significant change in expression after MCAo. The GluA2 subunit, the protein product of the *Gria2* gene, is crucial for the Ca²⁺ permeability of the AMPA receptors and, for example, in cerebellar Bergmann glia this subunit is absent (Hollmann et al. 1991; Burnashev et al. 1992). The *Gria3* gene was expressed in 4 % of the control cells; however, in D7 and D14 cells its expression was significantly increased (43 and 50 %, respectively). The *Gria4* gene was expressed in 10 % of the control cells, while the number of cells expressing this gene increased to 51 % in D7 cells and to 49 % in D14 cells. Thus, after MCAo, the gene expression of 3 out of 4 AMPA receptor subunits was increased at least fourfold.

A similar trend was observed with genes coding kainate receptor subunits. The numbers of cells expressing *Grik1,2,3,4,5* were increased 10-, 3-, 9-, 15-, and 2-fold after MCAo. The maximum expression of *Grik3,4* was observed in D7 cells and that of *Grik1,2,5* in D14 cells.

The expression of genes coding the subunits of NMDA receptors underwent dramatic changes as well. The *Grin1* gene was present in 7 % of the control cells, and this number was increased to 30 % in D7 and 43 % in D14 cells. From among all of the *Grin2* genes, the only gene that displayed a significant increase in the number of expressing cells after MCAo was *Grin2d*. The *Grin3a* gene, which codes the recently discovered GluN3A subunit of NMDA receptors with a prominent effect on the Mg²⁺ block and Ca²⁺ permeability of NMDA receptors (Perez-

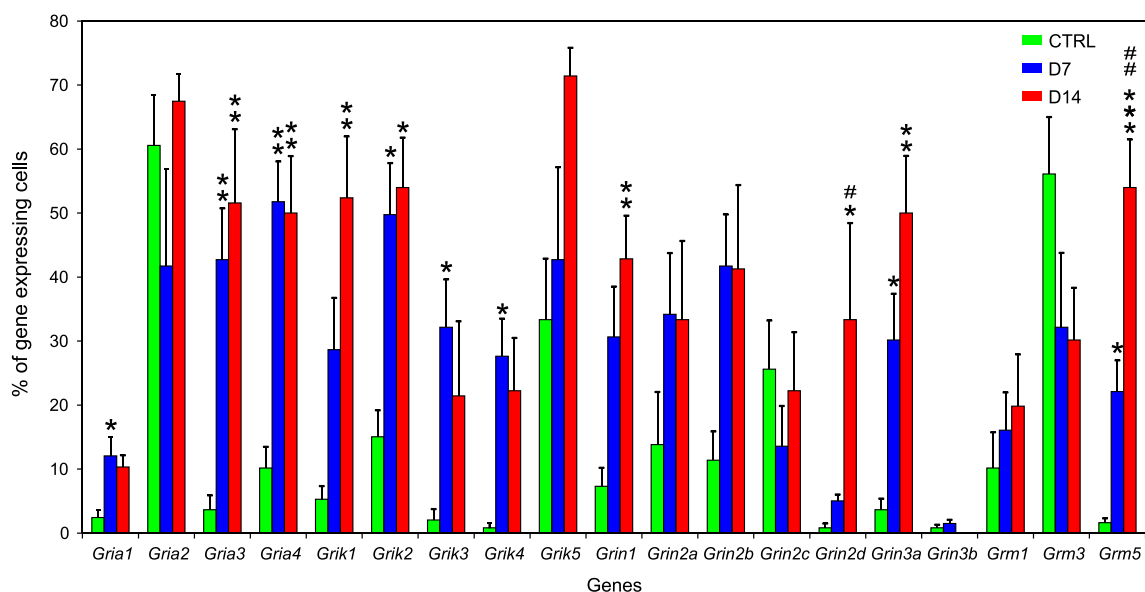


Fig. 1 The percentage of cells expressing genes coding individual subunits of glutamate receptors in control mice and in mice after MCAo. Cells isolated from control mice (CTRL, 5 mice, 246 cells) and from mice 7 and 14 days after MCAo (D7, 4 mice, 196 cells and D14, 3 mice, 125 cells) were used. Genes coding AMPA receptors (*Gria1-4*), kainate receptors (*Grik1-5*), NMDA receptors (*Grin1-3b*),

and metabotropic glutamate receptors (*Grm1,3,5*) were studied. Error bars represent SEM. Significant differences between D7/D14 compared to CTRL (* $p < 0.05$, ** $p < 0.01$, *** $p < 0.001$) and D14 compared to D7 (# $p < 0.05$, ## $p < 0.01$) were calculated by one-way ANOVA followed by the Bonferroni post-test

Otano et al. 2001; Cavara and Hollmann 2008), was expressed in 7–12-fold more cells isolated from mice after ischemic insult when compared to control cells (30 % of D7 and 50 % of D14 cells compared to 4 % in control cells). The expression of the *Grin3b* gene was very low; we detected it only in 1 % of control cells and 2 % of D7 cells, while there was no expression in D14 cells.

Together with ionotropic glutamate receptors, we also studied the expression of genes coding the most abundant metabotropic receptor subunits in glial cells *Grm1,3,5* (D'Antoni et al. 2008). Ten percent of control cells expressed *Grm1*, and this incidence did not significantly change after MCAo. The number of cells expressing *Grm3* shifted from 56 % in control cells to 30–32 % after MCAo. The largest increase in the percentage of cells expressing a particular gene after MCAo was observed with *Grm5*, which was detected in only 1.6 % of the control cells. Following ischemic injury, its expression increased 13-fold in D7 cells and 33-fold in D14 cells. This is in accordance with other studies showing the absence of *Grm5* in adult astrocytes under physiological conditions (Sun et al. 2013) and an increased presence of *Grm5* mRNA and mGluR5 protein in reactive astrocytes (Ulas et al. 2000; Aronica et al. 2000). Moreover, *Grm5* together with *Grin2d* was the only genes with significantly increased expression in D14 cells when compared to D7 cells.

Gene Expression Profiling of Distinct Subpopulations of GFAP/EGFP⁺ Cells

There have been several recent studies demonstrating the heterogeneity of GFAP/EGFP⁺ cells (Serrano et al. 2008; Ståhlberg et al. 2011; Benesova et al. 2012; Rusnakova et al. 2013). The single-cell RT-qPCR method used in this work is suitable for studying such heterogeneity, since it provides information about the gene expression levels of several genes in individual cells, with the possibility to further analyze the division of the cells into subpopulations. In this study, PCA was used to find three distinct subpopulations (SP1–SP3) among a pool of control, D7, and D14 cells (Fig. 2a). The SOM analysis, which forced the division of the cells into three groups, confirmed the stable classification of these subpopulations. The division into subpopulations was performed according to the similarity in gene expression of glial cell markers (*Cspg4*, *Pdgfra*, *Slc1a3*, *Glul*, *Gfap*, *Aqp4*) and glutamate receptor subunits (*Gria1–4*, *Grik1–5*, *Grin1–3b*, *Grm1,3,5*). There was an interesting tendency in the representation of control, D7, and D14 cells in these subpopulations (Fig. 2b). Subpopulation SP1 mostly comprised control cells, SP2 contained 30 % of control cells but mostly D7 cells, and SP3 was formed almost solely by cells after MCAo (42 %

of D7 cells and 54 % of D14 cells). From the bar plot showing the expression levels of genes in the SP1–SP3 subpopulations (Fig. 2c), it is evident that the highest gene transcript levels were in subpopulation SP3, which consisted especially of D7 and D14 cells, indicating the importance of glutamate receptors after ischemia. This also corresponded with the increased percentage of cells expressing genes coding glutamate receptors after MCAo (Fig. 1).

Spearman Correlation Coefficients

Even though there is heterogeneity among GFAP/EGFP⁺ cells, there were still some trends in gene expression patterns when comparing control, D7, and D14 cells. In the next step, we focused on a detailed classification of control cells and those isolated at particular times after MCAo. For this purpose, the Spearman correlation coefficients between pairs of genes were calculated; all of the correlation coefficients are shown in Online Resource 1. Since some of the GFAP/EGFP⁺ cells also expressed genes coding the NG2 glial markers *Cspg4* and/or *Pdgfra* as previously shown (Rusnakova et al. 2013), we were able to assess significant correlations between genes coding glutamate receptors and glial cells markers (Fig. 3).

The lowest number of correlations was observed in control cells. Six genes (*Gria1*, *Gria3*, *Grik5*, *Grin2d*, *Grin3b*, and *Grm5*) did not correlate with any glial marker in this group, while the remaining 13 genes correlated positively with at least one NG2 glial marker. Positive correlations with at least 2 out of 4 astrocytic markers were observed only with 3 genes (*Gria2*, *Grin2c*, and *Grm3*), whereas negative correlations were found with 4 genes (*Gria4*, *Grik3*, *Grin2a*, and *Grm1*). In control cells, we can summarize that most of the glutamate receptors were especially present in GFAP/EGFP⁺ cells, which expressed NG2 glial markers.

The correlation coefficients in D7 cells showed a strong positive correlation of AMPA and kainate receptor subunits with NG2 glial markers, which was not true for NMDA receptor subunits (a positive correlation with only *Grin1*, *Grin3a*, and marginally *Grin2d*) and metabotropic glutamate receptors (a positive correlation with *Grm5* only). In contrast to control cells, almost all glutamate receptor subunits displayed a positive correlation with astrocytic markers in D7 cells. Surprisingly, a positive correlation was also observed between the astrocytic marker *Slc1a3* and the NG2 glial markers *Cspg4* and *Pdgfra* (see Online Resource 1), which reflects the complex changes accompanying reactive astrogliosis after an ischemic insult.

In D14 cells, the situation was much more comprehensible. There was no positive correlation between genes

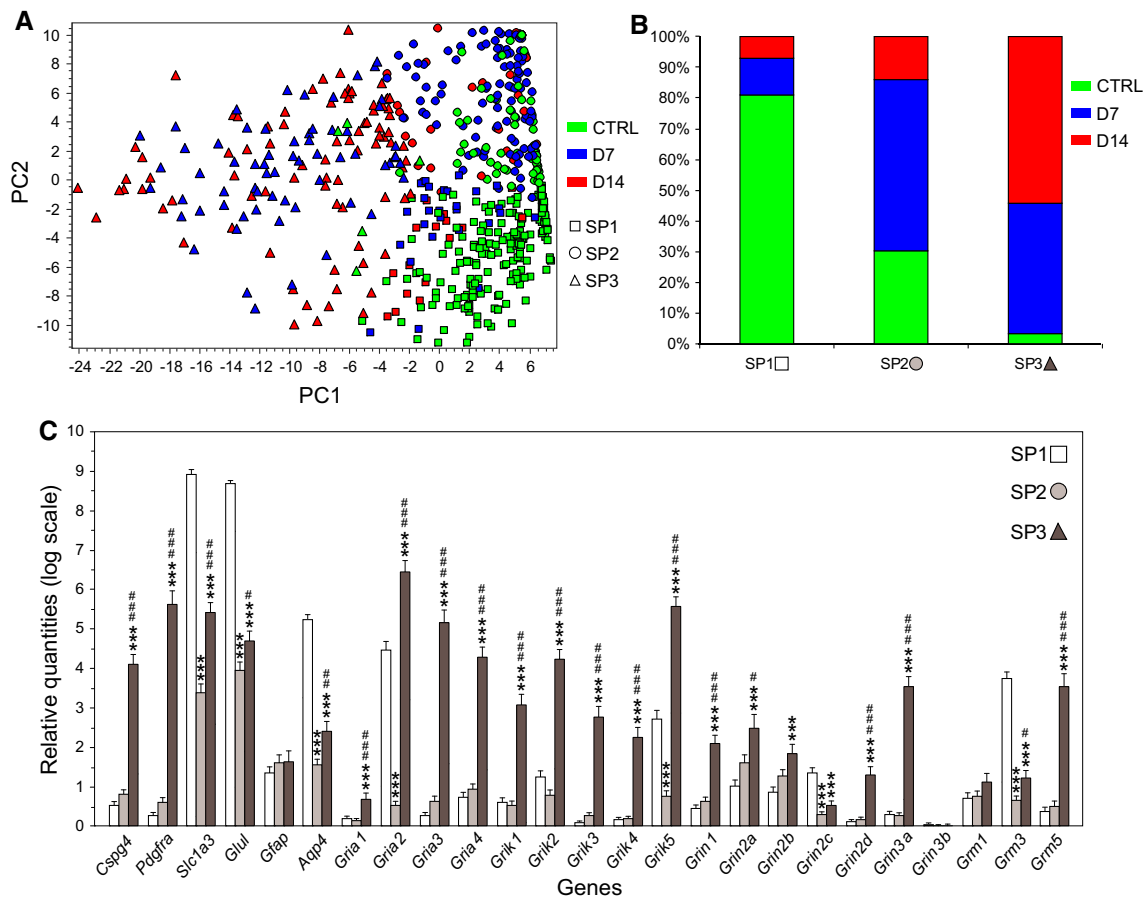


Fig. 2 Gene expression profiling of distinct subpopulations of GFAP/EGFP⁺ cells isolated from the cortex of GFAP/EGFP⁺ mice. **a** Principal component analysis (PCA) of cells from control mice (CTRL, 246 cells/5 mice) and those 7 and 14 days after MCAo (D7, 199 cells/4 mice; D14, 126 cells/3 mice). The data were mean-centered according to the genes. The cells were divided into three groups by Kohonen self-organizing maps (SOM) and are marked by different symbols (*squares* for subpopulation SP1, *circles* for

subpopulation SP2, and *triangles* for subpopulation SP3). **b** Percentage representation of CTRL, D7, and D14 cells in the subpopulations SP1–3. **c** Bar plot with SEM showing the relative expression of the analyzed genes in subpopulations SP1–3. Significant differences between SP2/SP3 compared to SP1 (***p* < 0.001) and SP3 compared to SP2 ([#]*p* < 0.05, ^{##}*p* < 0.01, ^{###}*p* < 0.001) were calculated by one-way ANOVA followed by the Bonferroni post-test

coding NG2 glial and astrocytic markers (see Online Resource 1), and also most of the genes coding glutamate receptor subunits correlated positively only with NG2 glial or astrocytic markers. For AMPA receptors, the correlation coefficients were similar to those in control cells. The only difference was with the *Gria3* gene, which was positively correlated with astrocytic markers in D14 cells. Kainate receptors also showed a similar trend as in control cells, since they were mostly correlated with NG2 glial markers. Intriguingly, NMDA and metabotropic glutamate receptors showed a very distinct correlation pattern, as *Grin2a-d* and *Grm3,5* showed a strong negative correlation with NG2 glial markers and a positive correlation with astrocytic markers. The only genes coding NMDA receptor subunits that positively correlated with NG2 glial markers were *Grin1* and *Grin3a*.

Immunohistochemical Analysis of NMDA Receptor Subunits

The single-cell RT-qPCR studies provided us with information about the levels of mRNA transcripts in single cells. As the next step, we performed an immunohistochemical analysis to verify that these transcripts were translated into proteins. For this analysis, we chose NMDA receptors since there are many unresolved questions about their presence and function in glial cells (Dzamba et al. 2013).

The immunohistochemical analysis (Fig. 4) showed staining of cortical GFAP/EGFP⁺ glial cells for individual NMDA receptor subunits (GluN1, GluN2A-D, and GluN3A-B) in tissue slices from controls and from mice 14 days after MCAo, in which the images were taken from

CTRL							D7							D14						
	Cspg4	Pdgfra	Slc1a3	Glul	Gfap	Aqp4		Cspg4	Pdgfra	Slc1a3	Glul	Gfap	Aqp4		Cspg4	Pdgfra	Slc1a3	Glul	Gfap	Aqp4
Gria1							Gria1	0,28	0,28	0,31	0,16			Gria1						
Gria2	0,19		0,28	0,47		0,45	Gria2	0,60	0,56	0,48	0,14		0,20	Gria2	0,41	0,45	0,28			
Gria3							Gria3	0,66	0,65	0,46			0,15	Gria3			0,28	0,31		
Gria4	0,19		-0,13	-0,13			Gria4	0,50	0,51	0,39			0,15	Gria4	0,39	0,48				-0,25
Grik1	0,18	0,35					Grik1	0,37	0,37	0,36	0,14		0,23	Grik1	0,22	0,29	0,32			
Grik2	0,20				0,16		Grik2	0,45	0,44	0,30	0,27	-0,15	0,15	Grik2	0,39	0,42				-0,19
Grik3		0,29	-0,18	-0,16		-0,14	Grik3	0,53	0,50	0,25				Grik3	0,37	0,32				-0,28
Grik4	0,22	0,23					Grik4	0,51	0,50	0,34				Grik4	0,36	0,48		-0,20		-0,25
Grik5							Grik5	0,43	0,44	0,48	0,31		0,34	Grik5	0,31	0,37	0,37	0,27		
Grin1	0,30				0,14		Grin1	0,30	0,21	0,19			0,19	Grin1	0,23	0,23				
Grin2a	0,23		-0,34	-0,22		-0,13	Grin2a			0,17	0,20	0,22	0,17	Grin2a	-0,45	-0,42	0,37	0,54		0,25
Grin2b	0,16		-0,14				Grin2b							Grin2b	-0,24	-0,20				0,27
Grin2c	0,14			0,18		0,21	Grin2c			0,14	0,25		0,28	Grin2c	-0,24	-0,25	0,42	0,36		0,42
Grin2d							Grin2d	0,17				-0,19		Grin2d	-0,26	-0,21		0,20		0,24
Grin3a	0,19	0,30					Grin3a	0,63	0,67	0,51			0,17	Grin3a	0,55	0,62	0,18			
Grin3b							Grin3b							Grin3b						
Grm1	0,18		-0,25	-0,23		-0,13	Grm1					0,15	0,22	Grm1				0,21		0,27
Grm3		0,16	0,25	0,46		0,40	Grm3			0,27	0,48	0,28	0,35	Grm3	-0,24	-0,27	0,50	0,54		0,47
Grm5							Grm5	0,50	0,46	0,25				Grm5	-0,30	-0,24	0,47	0,55		0,20

Fig. 3 Spearman correlation coefficients between genes coding glutamate receptor subunits and markers of NG2 glia/astrocytes in control cells (CTRL) and in cells 7 and 14 days after MCAo (D7, D14). The correlation coefficients were calculated from all cells including those without any expression of the studied genes. Positive

correlations are highlighted in *green*, negative in *red*. All the values of the correlation coefficients are significant with $p < 0.05$. Correlation coefficients with $p < 0.001$ are in *bold* (Complete list of Spearman correlation coefficients is provided in Online Resource 1)

the ischemic rim (Fig. 4b). The analysis revealed that there were GFAP/EGFP⁺ cells positively stained for the GluN3A subunit in controls; however, we did not observe any GFAP/EGFP⁺ glial cells positively stained for other NMDA receptor subunits under control conditions. In contrast, 14 days after MCAo, we observed GFAP/EGFP⁺ cells positive for the NMDA receptor subunits GluN1, GluN2B-D, and GluN3A close to the ischemic lesion. Immunohistochemical staining for the GluN2A subunit differed from that of the rest of the subunits since none of the GFAP/EGFP⁺ cells were positive for GluN2A; the only positive cells morphologically resembled neurons. As for the GluN3B immunostaining, there were positive cells in subcortical regions (data not shown), but none of the cells in the cortex were positive, which correlates with the single-cell RT-qPCR results. Nonetheless, the immunohistochemical analysis revealed that especially after ischemia, many GFAP/EGFP⁺ cells became positive for most of the NMDA receptor subunits.

NMDA Receptors in GFAP/EGFP⁺ Glial Cells – Ca²⁺ Imaging Measurements In Situ

Based on the results obtained from single-cell RT-qPCR and immunohistochemical analysis, we also performed a functional study of NMDA receptors in GFAP/EGFP⁺ glial cells using a Ca²⁺ imaging measurement technique. The experiments were carried out in tissue slices prepared from

GFAP/EGFP mice, either in controls or mice 13–14 days after MCAo (D13–14 mice).

First of all, we aimed to clarify what is the delay of the NMDA-evoked Ca²⁺ responses and to what extent are NMDA-evoked intracellular Ca²⁺ elevations dependent on agonist concentration. The average delay of the onset of Ca²⁺ responses following an application of 100 μM NMDA was 32.4 s (Fig. 5a). Moreover, the Ca²⁺ responses also differed in their kinetics; they displayed a large variability ranging from fast transient Ca²⁺ spikes to gradual changes of Ca²⁺ concentration indicating sustained Ca²⁺ entry. As expected, the Ca²⁺ elevations increased with the concentration of NMDA applied, as 4 μM and 20 μM NMDA-evoked responses were lower by 78 and 42 %, respectively, when compared to the application of 100 μM NMDA (Fig. 5b). The distribution of Ca²⁺ responses evoked by 100 μM NMDA did not reveal any heterogeneity in the magnitude of the responses (Fig. 5c). The co-application of 1 μM TTX did not result in any significant decrease in the Ca²⁺ responses evoked by 100 μM NMDA (Fig. 5d). The responses to the application of 100 μM NMDA were sensitive to the selective NMDA receptor antagonist DL-APV, which markedly blocked Ca²⁺ elevations (Fig. 5e). To clarify the subunit composition of the NMDA receptors, we further tested the effect of 10 μM memantine, which is a very efficient inhibitor of GluN2C- and GluN2D-containing NMDA receptors. The co-application of memantine led to a significant diminishing of the

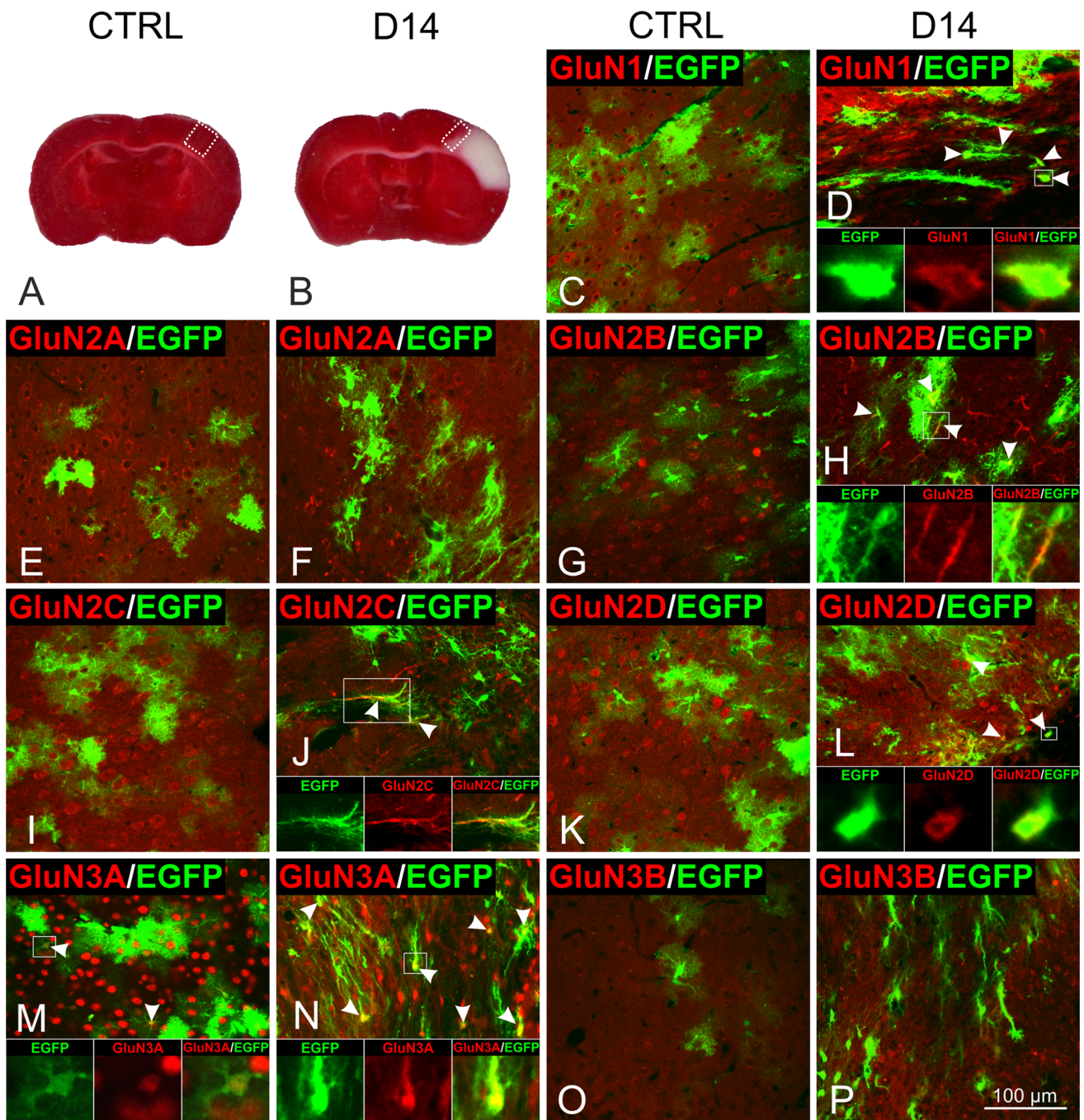


Fig. 4 Immunohistochemical analysis of the GluN1, GluN2A–D, and GluN3A–B subunits of the NMDA receptors in the cortex of adult GFAP/EGFP mice under control conditions (CTRL) and 14 days after MCAo (D14). Coronal brain sections from CTRL (a) and D14 (b) animals stained with triphenyl tetrazolium chloride. The white color in b indicates the volume of ischemic tissue at D14. The boxed areas indicate the regions in which the immunohistochemical analysis

was performed. The arrowheads in c–p indicate the overlay of GFAP/EGFP⁺ cells and NMDA subunit staining—see figure insets for detailed images of cells in white rectangles. Note the overlap of the EGFP signal with GluN3A staining in CTRL tissue and GluN1, GluN2B–D, and GluN3A staining at D14. The same scale bar applies to all non-inset images

NMDA-evoked Ca²⁺ elevations (Fig. 5f). On the other hand, the co-application of NBQX (AMPA and kainate receptors antagonist) and PPADS (P2X receptors antagonist) did not cause any changes (data not shown).

To study the impact of MCAo, we compared the Ca²⁺ responses in control and D13–14 mice (Fig. 5g). The application of 100 μM NMDA evoked a markedly lower Ca²⁺ influx in the GFAP/EGFP⁺ cells after MCAo. We

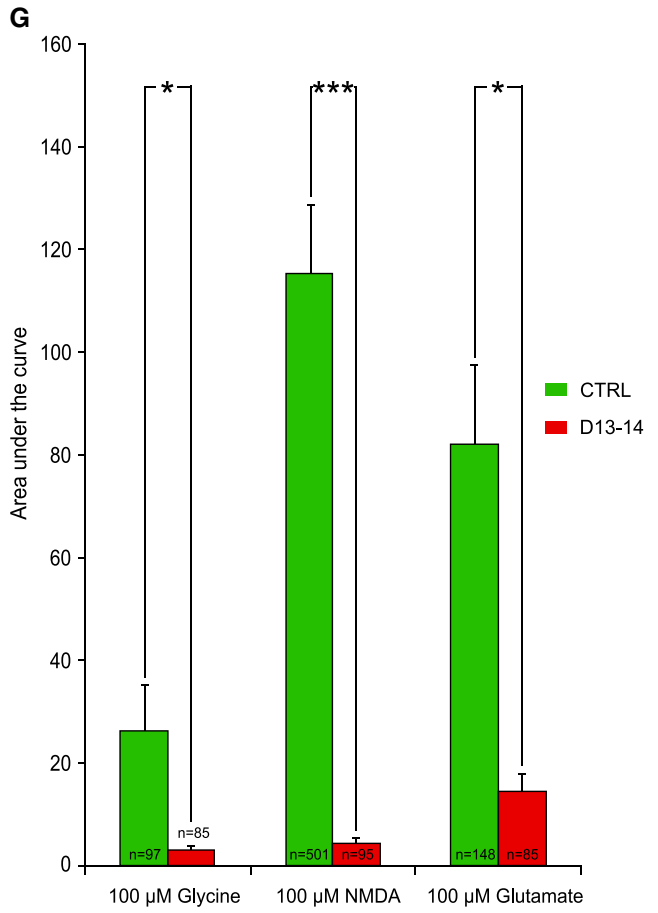
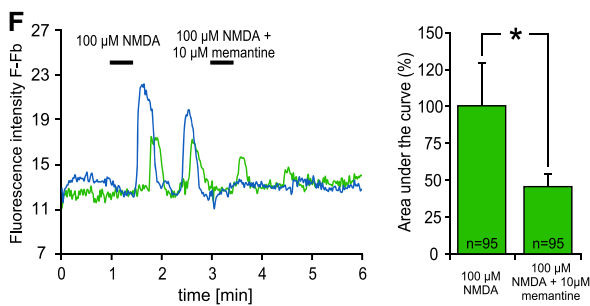
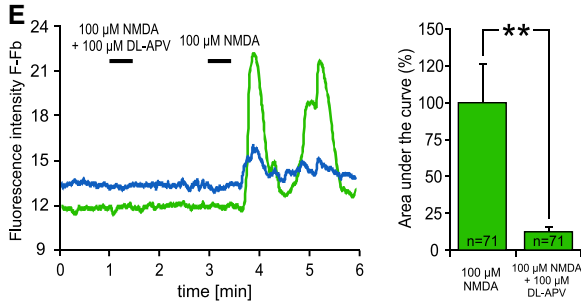
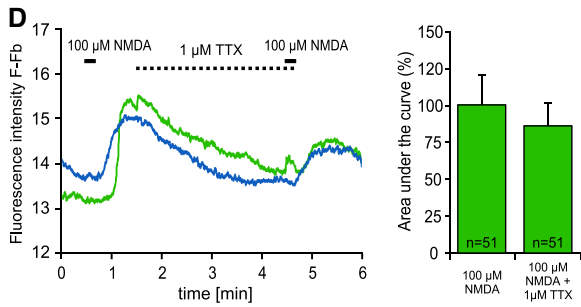
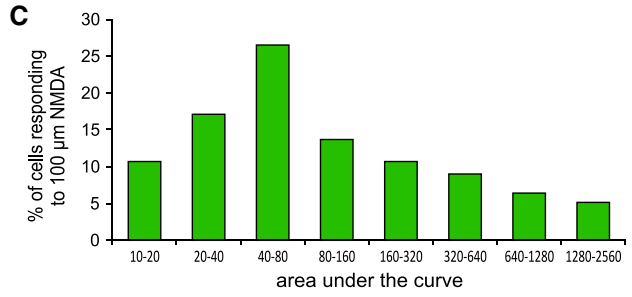
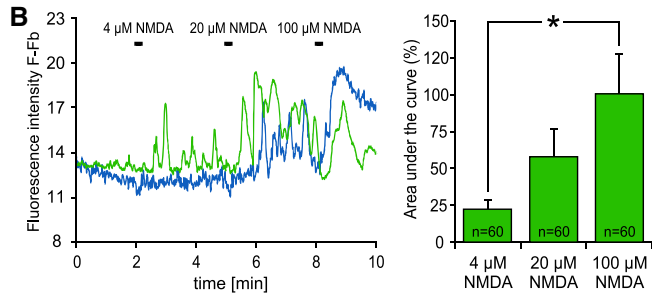
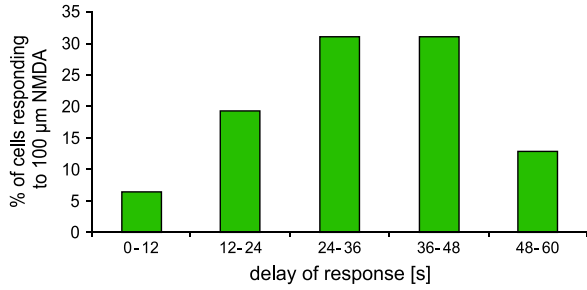
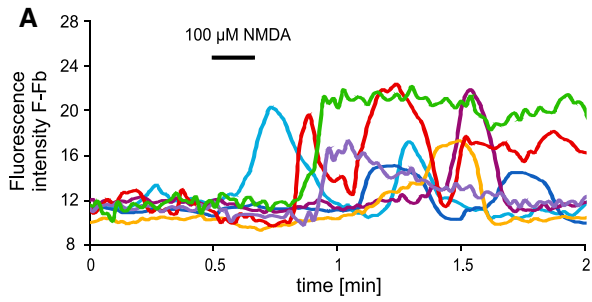


Fig. 5 Calcium imaging measurements of cortical GFAP/EGFP⁺ glial cells from GFAP/EGFP mice in situ. **a** Kinetics of the responses to the application of 100 μM NMDA (*top*). Quantification of the delay of the response onset shows that the average delay was ~30 s (*bottom*) ($n = 94$). **b** The concentration dependence of control cells responding to the application of NMDA (4, 20, and 100 μM, *left*) with quantification of the responses (*right*). **c** A histogram of the distribution of Ca²⁺ responses evoked by the application of 100 μM NMDA. Only cells with responses having an area under the curve higher than ten were analyzed ($n = 232$). **d** The co-application of 1 μM TTX did not reveal any significant change in the Ca²⁺ responses evoked by 100 μM NMDA. **e** The selective NMDA receptor blocker DL-APV markedly blocked the Ca²⁺ elevations evoked by the application of 100 μM NMDA. **f** The co-application of memantine decreased the NMDA-evoked Ca²⁺ elevation, which indicates the presence of GluN2C–D subunits in the NMDA receptors. **g** A comparison of the Ca²⁺ responses to the application of 100 μM glycine, 100 μM NMDA, and 100 μM glutamate in control cells (CTRL) and in cells 13–14 days after MCAo (D13–14). *Error bars* represent SEM. Significant differences ($*p < 0.05$, $**p < 0.01$, and $***p < 0.001$) were calculated by one-way ANOVA followed by the Bonferroni post-test (**b**), a paired *t* test (**d–f**), and an unpaired *t* test (**g**); n indicates the number of cells

suggest that this might be due to the increased presence of the GluN3A subunit in NMDA receptors after MCAo, which leads to lower Ca²⁺ permeability of NMDA receptors (Perez-Otano et al. 2001; Cavara and Hollmann 2008). The application of 100 μM glycine or 100 μM glutamate followed the same trend as they both evoked lower responses in D13–14 cells when compared to controls (Fig. 5g).

NMDA Receptors in GFAP/EGFP⁺ Glial Cells – Ca²⁺ Imaging Measurements In Vitro

It is well known that recordings in situ are affected by interactions between cells, particularly by neuron-glia interactions. To address this issue, we characterized the NMDA responses in individual GFAP/EGFP⁺ glial cells isolated from the somatosensory cortices of control or D13–14 mice and cultured for 5–6 days. The NMDA receptor co-agonist glycine was routinely added to the application of NMDA at 100 μM concentration in in vitro measurements since there was no endogenous source of glycine, but its addition did not cause any significant differences. The kinetics of the Ca²⁺ responses in the cultured cells was different from those recorded in situ. In 77 % of cells, the responses occurred within 12 s following the application of 500 μM NMDA with 100 μM glycine (95 % within 24 s), and fast transient Ca²⁺ spikes were not observed (Fig. 6a). To confirm the specificity of the NMDA responses, we used 100 μM DL-APV, which blocked the Ca²⁺ responses evoked by 500 μM NMDA with 100 μM glycine in all tested cells (data not shown). The ischemic insult had a significant impact on NMDA-evoked responses as only

8.4 % of cells isolated from the injured cortical tissue of D13–14 mice responded to the application of 500 μM NMDA with 100 μM glycine compared to 33.5 % of cells isolated from controls (Fig. 6b). The diminished intracellular Ca²⁺ elevations after NMDA application observed in situ in post-ischemic GFAP/EGFP⁺ glial cells were thus preserved even after 5–6 days of in vitro cultivation. Since in vitro Ca²⁺ imaging enabled the measurement of Ca²⁺ responses from single cells at much better resolution than in situ, in large ramified cells we observed that the responses to the application of 500 μM NMDA with 100 μM glycine did not occur uniformly in all of the processes, but were present in only some of the processes (Fig. 6c).

Discussion

In the present work, we have shown that post-ischemic glial cells undergo marked changes in the expression of subunits of ionotropic as well as metabotropic glutamate receptors. Our immunohistochemical analyses confirmed the presence of NMDA receptor subunits in GFAP/EGFP⁺ glial cells, and Ca²⁺ imaging measurements confirmed that changes in the expression of NMDA receptor subunits are also reflected in the functional properties of glial NMDA receptors.

The single-cell RT-qPCR technique provided us with information about the expression levels of 25 genes in single GFAP/EGFP⁺ glial cells under physiological conditions, but also following focal cerebral ischemia. Most of the genes coding subunits of glutamate receptors increased their expression after MCAo, and the largest increase was observed in *Grm5*. This is an interesting result since the mGluR5 receptor, coded by the *Grm5* gene, is crucial in modulating neuronal activity and in the functioning of tripartite synapses. Our result is in accordance with a recent study showing that the expression of *Grm5* in astrocytes was undetectable after postnatal week 3, in contrast to *Grm3* which was expressed at all developmental stages (Sun et al. 2013). In the current work, we show that the number of GFAP/EGFP⁺ glial cells expressing the *Grm1* and *Grm3* genes did not significantly change after MCAo; however, *Grm5* became detectable in the majority of these cells, which indicates the importance of this receptor in post-ischemic glia. Since the activation of mGluR5 receptors was shown to result in glutamate, ATP and/or D-serine release from glial cells, they might modulate neuronal activity in the post-ischemic brain (Haydon and Carmignoto 2006). However, mGluR5 receptors were also shown to modulate the expression and function of glutamate transporters in glia and thus participate in regulating extracellular glutamate concentration (Aronica et al. 2003; Vermeiren et al. 2005; D'Antoni et al. 2008). Another

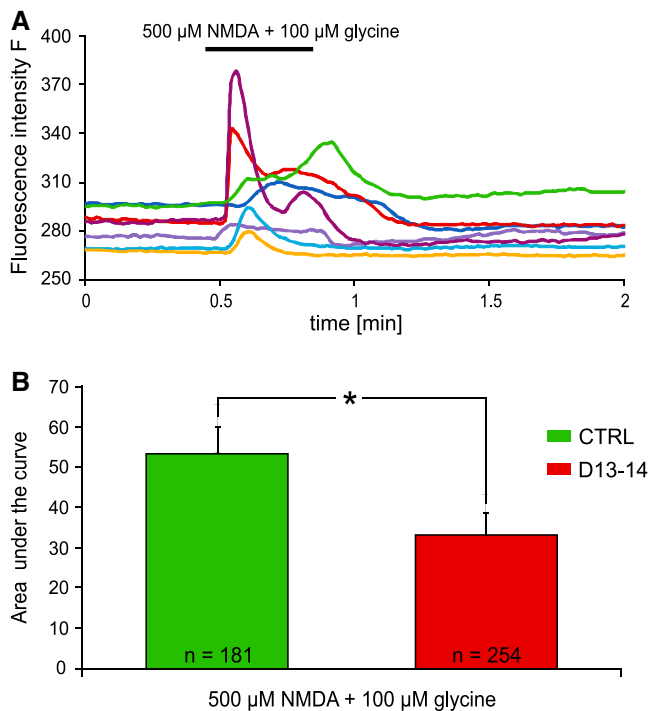
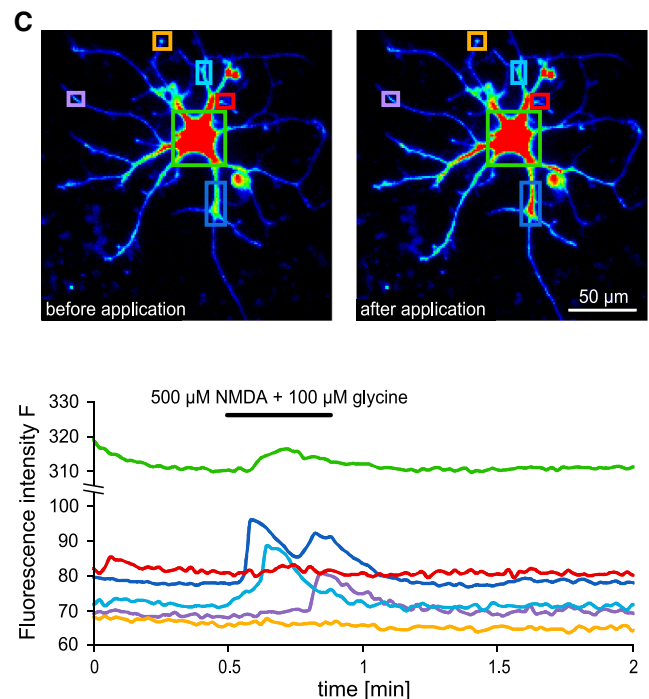


Fig. 6 Calcium imaging measurements of cortical GFAP/EGFP⁺ glial cells from GFAP/EGFP mice in vitro. **a** Kinetics of the responses to the application of 500 μM NMDA + 100 μM glycine. **b** A comparison of the Ca²⁺ responses to the application of 500 μM NMDA + 100 μM glycine in cells isolated from control mice (CTRL) and those isolated from mice 13–14 days after MCAO (D13–14). Error bars represent SEM. Asterisk indicates a significant

interesting result was regarding the *Gria2* gene, which was present in 61 % of control cells, a result that did not significantly change after MCAO. This subunit is crucial for Ca²⁺ permeability of AMPA receptors as its presence markedly diminishes their Ca²⁺ permeability (Hollmann et al. 1991; Burnashev et al. 1992). As for the NMDA receptors, the presence of genes coding NMDA receptor subunits was increased in cells after MCAO when compared to controls. The role of NMDA receptors in glial cells is still not fully elucidated, and our data might contribute to unraveling their function, which is presumably also involved in CNS pathologies, such as ischemia or tumors (Aronica et al. 2001). One of their possible roles could be the activation of survival signaling pathways (Hetman and Kharebava 2006) or, as recently shown, astrocytic NMDA receptors can control the exocytosis of gliotransmitters and thus control synaptic transmission and plasticity (Lalo et al. 2014). It is also worth noting that there were 356 cells that expressed at least one gene coding a NMDA receptor subunit in our study, and 236 of them did not express the *Grin1* gene encoding the GluN1 subunit, which according to current knowledge is obligatory in NMDA receptor formation. A similar result was reported



difference ($p < 0.05$) calculated by an unpaired *t* test; *n* indicates the number of cells. **c** Imaging of the Ca²⁺ elevation induced by the application of 500 μM NMDA + 100 μM glycine with a focus on the cell processes. Traces in different colors (bottom) correspond to the imaged regions in the image of the GFAP/EGFP⁺ glial cell (top). Note that Ca²⁺ elevations were not detected in all of the processes

by Cahoy and colleagues, who reported the presence of *Grin2c* and *Grin3a* but the absence of *Grin1* in cortical astrocytes (Cahoy et al. 2008). This might be due to the high protein stability of the GluN1 subunit compared to the GluN2-3 subunits as previously reported (Atlason et al. 2007). Moreover, there are indications that murine NMDA receptors can be also co-assembled without the GluN1 subunit (Perez-Otano et al. 2001; Matsuda et al. 2003), but their functional properties are debatable.

The division of control, D7, and D14 cells into three subpopulations according to their gene expression showed that D7 and especially D14 cells have the highest relative expression of most of the genes coding subunits of glutamate receptors (subpopulation SP3), which distinguishes them from control cells. However, in subpopulation SP2, formed mainly by D7 but also by D14 cells, the relative expression of glutamate receptor subunits is lower, indicating that cells after MCAO are not homogeneous.

Interesting results were obtained from the Spearman correlation coefficient analysis between genes in control, D7, and D14 cells. Since we used a GFAP/EGFP⁺ glial cell population in this study, which among astrocytic markers expressed also NG2 glial markers in some cells, we were

able to study the correlations between particular genes coding glutamate receptor subunits with genes coding markers of astrocytes and NG2 glia. Most of the AMPA receptors are heterotetrameric, consisting of two GluA2 and two GluA1, GluA3, or GluA4 subunits. Since *Gria2* correlated positively with astrocytic and NG2 glial markers, our results indicate that the presence of AMPA receptors is without any preference to these markers. An interesting situation was observed in D14 cells, since *Gria3* positively correlated with astrocytic markers, indicating AMPA receptors of GluA2/GluA3 type in these cells, and *Gria4* correlated with NG2 glial markers, indicating AMPA receptors of GluA2/GluA4 type in these cells (Fig. 3). Several studies have shown that astrocytes possess kainate receptors (Seifert and Steinhäuser 2001; Brand-Schieber et al. 2004), which we also showed in the current work. Moreover, our results suggest that genes coding kainate receptor subunits correlated mostly with those GFAP/EGFP⁺ cells that expressed NG2 glial markers, which would also confirm the results of a study demonstrating functional kainate receptors in NG2 glia (Kukley and Dietrich 2009; Haberlandt et al. 2011). In D7 cells, we observed a large positive correlation with astrocytic markers, but in D14 cells, most of the genes coding kainate receptor subunits again positively correlated with NG2 glial markers. An interesting correlation pattern was observed with genes coding NMDA receptor subunits. In control cells, these genes positively correlated mostly with NG2 glial markers; only *Grin1* and *Grin2c* were also partially correlated with astrocytic markers. In D7 cells, the number of NMDA subunits correlating with NG2 glial markers was reduced, and their correlation with astrocytic markers was increased. The most intriguing correlation pattern was found in D14 cells, where cells expressing NG2 glial markers were positively correlated with *Grin1* and *Grin3a* and moreover negatively correlated with *Grin2a-d*. This strongly indicates that 14 days after MCAo, the composition of NMDA receptors in the NG2 glial markers expressing GFAP/EGFP⁺ cells is of the GluN1/GluN3A type. On the other hand, *Grin2a-d* genes were positively correlated with astrocytic markers. As for the metabotropic glutamate receptors, control cells expressing astrocytic markers seemed to possess mGluR3 receptors but not mGluR1, whereas genes coding both of these receptors also partially correlated with NG2 glial markers. This situation changed completely in D14 cells, where genes coding metabotropic glutamate receptors positively correlated with astrocytic and negatively with NG2 glial markers.

To study glutamate receptors also on the protein level, we performed an immunohistochemical analysis of the entire set of the 7 currently known NMDA receptor subunits of GFAP/EGFP⁺ glial cells in the adult mouse cortex.

To the best of our knowledge, our analysis provides the first immunohistochemical evidence that GFAP/EGFP⁺ glial cells in the cortex possess GluN3A subunits, which has previously been discussed in many works (Verkhratsky and Kirchhoff 2007; Palygin et al. 2011; Kehoe et al. 2013). Under control conditions, we did not observe GFAP/EGFP⁺ cells positive for any NMDA receptor subunit, apart from GluN3A. This might be due to the fact that under control conditions, astrocytes have a bushy-like morphology with many fine processes. It was previously shown by electron microscopy that the GluN1 and GluN2A/B NMDA receptor subunits are present in astrocytes especially in the processes and not in the cellular bodies (Conti et al. 1996). The fluorescent immunohistochemical method is not able to distinguish NMDA receptor subunit positivity in fine processes from the background signal. On the other hand, reactive astrocytes present in the cortices of GFAP/EGFP mice 14 days after MCAo have a fibrous morphology with sharp edges separating them from the surrounding tissue, which enables the detection of positive staining for NMDA receptor subunits in these cells. Our immunohistochemical analysis clearly showed the positivity of cortical GFAP/EGFP⁺ cells for the GluN1, GluN2B-D, and GluN3A subunits 14 days after MCAo, which indicates the importance of NMDA receptors in glial cells under ischemic conditions. The GluN2A subunit was detected in cells that morphologically resembled neurons, but not in GFAP/EGFP⁺ cells. Since the single-cell RT-qPCR results indicate that GFAP/EGFP⁺ cells should contain this subunit, we hypothesize that it was not detected due to some post-translational modifications of the GluN2A protein or miRNA regulation, which might be specific to glia. In summary, the immunohistochemical analysis confirmed the presence of NMDA receptor subunits in GFAP/EGFP⁺ glial cells, especially after ischemia.

The NMDA receptors in GFAP/EGFP⁺ glial cells were also subjected to functional study utilizing a Ca²⁺ imaging technique. Calcium responses to the application of 100 μM NMDA were delayed in situ by ~30 s on average, as also reported in other studies (Serrano et al. 2008; Serrano et al. 2006; Porter and McCarthy 1995). We attribute this delay to the slow diffusion of NMDA in the brain tissue, which is supported by the fact that there were immediate responses in cultivated cells. There have been several studies showing a TTX-mediated partial reduction of NMDA-evoked responses (Schipke et al. 2001; Serrano et al. 2006, 2008). Similar to a study of oligodendrocytic NMDA receptors (Káradóttir et al. 2005), we did not observe any significant changes associated with the use of TTX, which might also be due to the fact that our application was relatively short and locally focused, in contrast to the above-mentioned studies showing a TTX-mediated effect (bath application for several minutes). As for the subunit composition of the

NMDA receptors, our results suggest a tri-heteromeric composition of the GluN1/GluN2C/GluN3A type. This is supported by the weak Mg^{2+} block observed for NMDA receptors containing the GluN3A subunit (Sasaki et al. 2002; Kehoe et al. 2013), as we observed Ca^{2+} elevations in aCSF that contained Mg^{2+} without the need for cell depolarization. Based on our single-cell RT-qPCR (Fig. 1) and immunohistochemical analyses (Fig. 4) showing low mRNA levels of *Grin3b* and the absence of GluN3B immunoreactivity, we do not assume the inclusion of the GluN3B subunit in the NMDA receptors. Di-heteromeric GluN1/GluN3A receptors have, however, no binding site for glutamate or NMDA, so the inclusion of the GluN2 subunit is also needed. Our data with memantine, which is an efficient inhibitor of GluN2C and GluN2D subunits (Kotermanski and Johnson 2009), suggest the incorporation of one of these subunits as well. Based on our single-cell RT-qPCR data, which show much higher expression of *Grin2c* in comparison to *Grin2d* in controls (Fig. 1), we suppose that at least in controls, the NMDA receptors contain mainly the GluN2C subunit. Nonetheless, we cannot exclude the possibility that GFAP/EGFP⁺ glial cells also possess GluN1/GluN2 NMDA receptors. We hypothesize that these could provide an amplification of the Ca^{2+} signal upon local depolarization, which would release the Mg^{2+} block. The application of NBQX and PPADS did not support the hypothesis that this local depolarization would be provided via AMPA, Kainate, or P2X receptors.

Both in situ and in vitro experiments showed that the application of NMDA evoked significantly lower Ca^{2+} elevations in GFAP/EGFP⁺ glial cells 13–14 days after MCAo when compared to control cells, which we hypothesize is due to the increased involvement of the GluN3A subunit as shown by our single-cell RT-qPCR and immunohistochemical analyses. The decreased Ca^{2+} permeability of NMDA receptors can be further caused by the incorporation of the GluN2D subunit in NMDA receptors (Burnashev et al. 1995; Paoletti 2011; Evans et al. 2012), which was also highly upregulated 14 days after MCAo. Another reason for decreased Ca^{2+} permeability of NMDA receptors might be their internalization, which was shown to be regulated by the particular subunit compositions (Lavezzari et al. 2004), and, for example, GluN3A internalization is regulated via phosphorylation of a tyrosine residue (Y971) within the GluN3A intracellular C-terminal tail (Chowdhury et al. 2013). Therefore, we cannot completely rule out the possibility that NMDA receptors in GFAP/EGFP⁺ glial cells are internalized or inactivated by the Ca^{2+} -calmodulin complex after MCAo (Ehlers et al. 1996). Interestingly, the Ca^{2+} permeability of astrocytic NMDA receptors after ischemia is region-specific, since as shown by Krebs and colleagues, acutely

isolated hippocampal astrocytes displayed NMDA-evoked Ca^{2+} elevations 20 days after global cerebral ischemia (Krebs et al. 2003). The number of cells responding to the application of 100 μ M glutamate in situ was also decreased after MCAo, but some Ca^{2+} influx was still detected, which is probably due to the presence of Ca^{2+} -permeable non-NMDA glutamate receptors. These could be ionotropic AMPA or kainate glutamate receptors (Burnashev et al. 1992), but also metabotropic mGluR5 glutamate receptors coded by the *Grm5* gene, which becomes strongly expressed in D14 cells and which mediates intracellular calcium elevations by releasing calcium from intracellular stores (Nakahara et al. 1997). In vitro cultivated GFAP/EGFP⁺ glial cells isolated from young adult mice enabled us to study NMDA-evoked responses in detail. Calcium imaging measurements revealed that the responses were process-specific, which corresponds with recent studies showing microdomains within astrocytic territories (Shigetomi et al. 2013). Moreover, this suggests that the response rates in our in situ experiments might be slightly underestimated since we recorded a signal only from the cellular body and not from the processes, where the responses probably originate (Schipke et al. 2001). The results obtained by Ca^{2+} imaging measurements thus supplement the data from single-cell RT-qPCR and immunohistochemical analysis and underline the changes of NMDA receptors in post-ischemic GFAP/EGFP⁺ glial cells.

In summary, our study provides an overall picture of ionotropic and metabotropic glutamate receptor expression in cortical GFAP/EGFP⁺ glial cells. We show how the expression of particular subunits of these receptors changes after focal cerebral ischemia. On the functional level, we further show that NMDA-mediated Ca^{2+} elevations significantly decrease after ischemia in GFAP/EGFP⁺ glial cells, which is presumably due to the involvement of the GluN3A subunit. We believe that our study thus adds a new piece of the puzzle to the picture, from which we will eventually understand all of the complex processes, including neuron-glia interaction or glutamate-mediated signaling, in glial cells and which might serve as a guide for research into precisely targeted therapeutics.

Acknowledgments This study was supported by the Grants GA CR P304/12/G069 and GACR 13-02154S from the Grant Agency of the Czech Republic, GAUK 604212 from the Grant Agency of the Charles University in Prague, CZ.1.05/1.1.00/02.0109 from the European Regional Development Fund, and CZ.1.07/2.3.00/30.0045 from the European Social Fund and the state budget of the Czech Republic.

Conflict of interest The authors declare that they have no conflict of interest.

References

- Aronica E, van Vliet EA, Mayboroda OA et al (2000) Upregulation of metabotropic glutamate receptor subtype mGluR3 and mGluR5 in reactive astrocytes in a rat model of mesial temporal lobe epilepsy. *Eur J Neurosci* 12:2333–2344
- Aronica E, Leenstra S, Jansen GH et al (2001) Expression of brain-derived neurotrophic factor and tyrosine kinase B receptor proteins in glioneuronal tumors from patients with intractable epilepsy: colocalization with N-methyl-D-aspartic acid receptor. *Acta Neuropathol* 101:383–392
- Aronica E, Gorter JA, Ijlst-Keizers H et al (2003) Expression and functional role of mGluR3 and mGluR5 in human astrocytes and glioma cells: opposite regulation of glutamate transporter proteins. *Eur J Neurosci* 17:2106–2118. doi:10.1046/j.1460-9568.2003.02657.x
- Atlas PT, Garside ML, Meddows E et al (2007) N-Methyl-D-aspartate (NMDA) receptor subunit NR1 forms the substrate for oligomeric assembly of the NMDA receptor. *J Biol Chem* 282:25299–25307. doi:10.1074/jbc.M702778200
- Benesova J, Rusnakova V, Honsa P et al (2012) Distinct expression/function of potassium and chloride channels contributes to the diverse volume regulation in cortical astrocytes of GFAP/EGFP mice. *PLoS One* 7:e29725. doi:10.1371/journal.pone.0029725
- Brand-Schieber E, Lowery SL, Werner P (2004) Select ionotropic glutamate AMPA/kainate receptors are expressed at the astrocyte-vessel interface. *Brain Res* 1007:178–182. doi:10.1016/j.brainres.2003.12.051
- Burnashev N, Khodorova A, Jonas P et al (1992) Calcium-permeable AMPA-kainate receptors in fusiform cerebellar glial cells. *Science* 256:1566–1570
- Burnashev N, Zhou Z, Neher E, Sakmann B (1995) Fractional calcium currents through recombinant GluR channels of the NMDA, AMPA and kainate receptor subtypes. *J Physiol* 485(Pt 2):403–418
- Cahoy JD, Emery B, Kaushal A et al (2008) A transcriptome database for astrocytes, neurons, and oligodendrocytes: a new resource for understanding brain development and function. *J Neurosci* 28:264–278. doi:10.1523/JNEUROSCI.4178-07.2008
- Castillo C, Norcini M, Martin Hernandez LA et al (2013) Satellite glia cells in dorsal root ganglia express functional NMDA receptors. *Neuroscience* 240:135–146. doi:10.1016/j.neuroscience.2013.02.031
- Cavara NA, Hollmann M (2008) Shuffling the deck anew: how NR3 tweaks NMDA receptor function. *Mol Neurobiol* 38:16–26. doi:10.1007/s12035-008-8029-9
- Chowdhury D, Marco S, Brooks IM et al (2013) Tyrosine phosphorylation regulates the endocytosis and surface expression of GluN3A-containing NMDA receptors. *J Neurosci* 33(9):4151–4164
- Conti F, DeBiasi S, Minelli A, Melone M (1996) Expression of NR1 and NR2A/B subunits of the NMDA receptor in cortical astrocytes. *Glia* 17:254–258. doi:10.1002/(SICI)1098-1136(199607)17:3<254:AID-GLIA7>3.0.CO;2-0
- D'Antoni S, Berretta A, Bonaccorso CM et al (2008) Metabotropic glutamate receptors in glial cells. *Neurochem Res* 33:2436–2443. doi:10.1007/s11064-008-9694-9
- Dzamba D, Honsa P, Anderova M (2013) NMDA receptors in glial cells: pending questions. *Curr Neuropharmacol* 11:250–262. doi:10.2174/1570159X11311030002
- Ehlers MD, Zhang S, Bernhardt JP, Huganir RL (1996) Inactivation of NMDA receptors by direct interaction of calmodulin with the NR1 subunit. *Cell* 84:745–755
- Evans RC, Morera-Herreras T, Cui Y et al (2012) The effects of NMDA subunit composition on calcium influx and spike timing-dependent plasticity in striatal medium spiny neurons. *PLoS Comput Biol* 8:e1002493. doi:10.1371/journal.pcbi.1002493
- Gottlieb M, Matute C (1997) Expression of ionotropic glutamate receptor subunits in glial cells of the hippocampal CA1 area following transient forebrain ischemia. *J Cereb Blood Flow Metab* 17:290–300. doi:10.1097/00004647-199703000-00006
- Haberlandt C, Derouiche A, Wyczynski A et al (2011) Gray matter NG2 cells display multiple Ca²⁺-signaling pathways and highly motile processes. *PLoS One* 6:e17575. doi:10.1371/journal.pone.0017575
- Haydon P, Carmignoto G (2006) Astrocyte control of synaptic transmission and neurovascular coupling. *Physiol Rev*. doi:10.1152/physrev.00049.2005
- Hetman M, Kharebava G (2006) Survival signaling pathways activated by NMDA receptors. *Curr Top Med Chem* 6:787–799
- Hollmann M, Hartley M, Heinemann S (1991) Ca²⁺ permeability of KA-AMPA-gated glutamate receptor channels depends on subunit composition. *Science* 252:851–853
- Honsa P, Pivonkova H, Dzamba D et al (2012) Polydendrocytes display large lineage plasticity following focal cerebral ischemia. *PLoS One* 7:e36816. doi:10.1371/journal.pone.0036816
- Káradóttir R, Cavalier P, Bergersen L, Attwell D (2005) NMDA receptors are expressed in oligodendrocytes and activated in ischaemia. *Nature* 438:1162–1166. doi:10.1038/nature04302. NMDA
- Kehoe LA, Bernardinelli Y, Muller D (2013) GluN3A: an NMDA receptor subunit with exquisite properties and functions. *Neural Plast* 2013:145387. doi:10.1155/2013/145387
- Kotermanski SE, Johnson JW (2009) Mg²⁺ imparts NMDA receptor subtype selectivity to the Alzheimer's drug memantine. *J Neurosci* 29:2774–2779. doi:10.1523/JNEUROSCI.3703-08.2009
- Krebs C, Fernandes HB, Sheldon C et al (2003) Functional NMDA receptor subtype 2B is expressed in astrocytes after ischemia in vivo and anoxia in vitro. *J Neurosci* 23:3364–3372
- Kukley M, Dietrich D (2009) Kainate receptors and signal integration by NG2 glial cells. *Neuron Glia Biol* 5:13–20
- Lalo U, Pankratov Y, Kirchhoff F et al (2006) NMDA receptors mediate neuron-to-glia signaling in mouse cortical astrocytes. *J Neurosci* 26:2673–2683. doi:10.1523/JNEUROSCI.4689-05.2006
- Lalo U, Palygin O, Rasooli-Nejad S et al (2014) Exocytosis of ATP from astrocytes modulates phasic and tonic inhibition in the neocortex. *PLoS Biol* 12:e1001747. doi:10.1371/journal.pbio.1001747
- Lavezzari G, McCallum J, Dewey CM et al (2004) Subunit-specific regulation of NMDA receptor endocytosis. *J Neurosci* 24(28):6383–6391
- Loane DJ, Stoica BA, Faden AI (2012) Metabotropic glutamate receptor-mediated signaling in neuroglia. *Wiley Interdiscip Rev Membr Transp Signal* 1:136–150. doi:10.1002/wmts.30
- Matsuda K, Fletcher M, Kamiya Y, Yuzaki M (2003) Specific assembly with the NMDA receptor 3B subunit controls surface expression and calcium permeability of NMDA receptors. *J Neurosci* 23:10064–10073
- Matthias K, Kirchhoff F, Seifert G et al (2003) Segregated expression of AMPA-type glutamate receptors and glutamate transporters defines distinct astrocyte populations in the mouse hippocampus. *J Neurosci* 23:1750–1758
- Nakahara K, Okada M, Nakanishi S (1997) The metabotropic glutamate receptor mGluR5 induces calcium oscillations in cultured astrocytes via protein kinase C phosphorylation. *J Neurochem* 69:1467–1475
- Nolte C, Matyash M, Pivneva T et al (2001) GFAP promoter-controlled EGFP-expressing transgenic mice: a tool to visualize astrocytes and astrogliosis in living brain tissue. *Glia* 33:72–86
- Palygin O, Lalo U, Pankratov Y (2011) Distinct pharmacological and functional properties of NMDA receptors in mouse cortical astrocytes. *Br J Pharmacol* 163:1755–1766. doi:10.1111/j.1476-5381.2011.01374.x

- Paoletti P (2011) Molecular basis of NMDA receptor functional diversity. *Eur J Neurosci* 33:1351–1365. doi:[10.1111/j.1460-9568.2011.07628.x](https://doi.org/10.1111/j.1460-9568.2011.07628.x)
- Perez-Otano I, Schulteis CT, Contractor A et al (2001) Assembly with the NR1 subunit is required for surface expression of NR3A-containing NMDA receptors. *J Neurosci* 21:1228–1237
- Porter JT, McCarthy KD (1995) GFAP-positive hippocampal astrocytes in situ respond to glutamatergic neuroligands with increases in $[Ca^{2+}]_i$. *Glia* 13:101–112
- Rusnakova V, Honsa P, Dzamba D et al (2013) Heterogeneity of astrocytes: from development to injury—single cell gene expression. *PLoS One* 8:e69734. doi:[10.1371/journal.pone.0069734](https://doi.org/10.1371/journal.pone.0069734)
- Sasaki YF, Rothe T, Premkumar LS et al (2002) Characterization and comparison of the NR3A subunit of the NMDA receptor in recombinant systems and primary cortical neurons. *J Neurophysiol* 87:2052–2063. doi:[10.1152/jn.00531.2001](https://doi.org/10.1152/jn.00531.2001)
- Schipke CG, Ohlemeyer C, Matyash M et al (2001) Astrocytes of the mouse neocortex express functional N-methyl-D-aspartate receptors. *FASEB J* 15:1270–1272
- Seifert G, Steinhäuser C (2001) Ionotropic glutamate receptors in astrocytes. *Prog Brain Res* 132:287–299. doi:[10.1016/S0079-6123\(01\)32083-6](https://doi.org/10.1016/S0079-6123(01)32083-6)
- Serrano A, Haddjeri N, Lacaille J-C, Robitaille R (2006) GABAergic network activation of glial cells underlies hippocampal heterosynaptic depression. *J Neurosci* 26:5370–5382. doi:[10.1523/JNEUROSCI.5255-05.2006](https://doi.org/10.1523/JNEUROSCI.5255-05.2006)
- Serrano A, Robitaille R, Lacaille J-C (2008) Differential NMDA-dependent activation of glial cells in mouse hippocampus. *Glia* 56:1648–1663. doi:[10.1002/glia.20717](https://doi.org/10.1002/glia.20717)
- Shigetomi E, Bushong EA, Hausteil MD et al (2013) Imaging calcium microdomains within entire astrocyte territories and endfeet with GCaMPs expressed using adeno-associated viruses. *J Gen Physiol* 141:633–647. doi:[10.1085/jgp.201210949](https://doi.org/10.1085/jgp.201210949)
- Ståhlberg A, Bengtsson M (2010) Single-cell gene expression profiling using reverse transcription quantitative real-time PCR. *Methods* 50:282–288. doi:[10.1016/j.ymeth.2010.01.002](https://doi.org/10.1016/j.ymeth.2010.01.002)
- Ståhlberg A, Andersson D, Aurelius J et al (2011) Defining cell populations with single-cell gene expression profiling: correlations and identification of astrocyte subpopulations. *Nucleic Acids Res* 39:e24. doi:[10.1093/nar/gkq1182](https://doi.org/10.1093/nar/gkq1182)
- Sun W, McConnell E, Pare J-F et al (2013) Glutamate-dependent neuroglial calcium signaling differs between young and adult brain. *Science* 339:197–200. doi:[10.1126/science.1226740](https://doi.org/10.1126/science.1226740)
- Ulas J, Satou T, Ivins KJ et al (2000) Expression of metabotropic glutamate receptor 5 is increased in astrocytes after kainate-induced epileptic seizures. *Glia* 30:352–361
- Verkhatsky A (2009) Neuronismo y reticulismo: neuronal-glia circuits unify the reticular and neuronal theories of brain organization. *Acta Physiol (Oxf)* 195:111–122. doi:[10.1111/j.1748-1716.2008.01926.x](https://doi.org/10.1111/j.1748-1716.2008.01926.x)
- Verkhatsky A, Kirchhoff F (2007) NMDA receptors in glia. *Neuroscientist* 13:28–37. doi:[10.1177/1073858406294270](https://doi.org/10.1177/1073858406294270)
- Vermeiren C, Najimi M, Vanhoutte N et al (2005) Acute up-regulation of glutamate uptake mediated by mGluR5a in reactive astrocytes. *J Neurochem* 94:405–416. doi:[10.1111/j.1471-4159.2005.03216.x](https://doi.org/10.1111/j.1471-4159.2005.03216.x)